NDT&E International 48 (2012) 10–15

Contents lists available at SciVerse ScienceDirect

NDT&E International

journal homepage: www.elsevier.com/locate/ndteint

Fatigue damage evaluation in A36 steel using nonlinear Rayleigh surface waves

Simon V. Walker [a], Jin-Yeon Kim [a], Jianmin Qu [b], Laurence J. Jacobs [a,c,*]

[a] School of Civil and Environmental Engineering, Georgia Institute of Technology, Atlanta, GA 30332, USA
[b] Department of Civil and Environmental Engineering, Northwestern University, Evanston, IL 60208, USA
[c] Woodruff School of Mechanical Engineering, Georgia Institute of Technology, Atlanta, GA 30332, USA

ARTICLE INFO

Article history:
Received 14 November 2011
Received in revised form
3 February 2012
Accepted 6 February 2012
Available online 13 February 2012

Keywords:
Nonlinear acoustics
Fatigue damage
Nonlinear Rayleigh waves

ABSTRACT

This research uses nonlinear Rayleigh waves to characterize the damage due to plastic deformation in A36 steel specimens subjected to quasi-static, monotonic tension, and low cycle fatigue. A36 steel is widely used in the civil infrastructure, such as steel bridges, where fatigue damage can lead to a catastrophic failure. Plastic deformation causes the generation of higher order harmonics in an initially monochromatic Rayleigh wave signal, and this measurable change occurs before macroscopic damage such as cracks appear in a specimen. This increase in the acoustic nonlinearity is produced by plasticity-induced microstructure changes, and thus can be taken as a direct measure of damage. Experiments are conducted using a pair of wedge transducers to generate and detect tone burst ultrasonic Rayleigh surface wave signals. The amplitudes of the first and second order harmonics are measured at different propagation distances to obtain the nonlinearity parameter for a given damage state throughout the fatigue life and monotonic loading process in three specimens. The results of the nonlinear ultrasonic measurements show an increase in the measured acoustic nonlinearity, especially in the early stages of fatigue life. In addition, there is a notably close relationship between the measured acoustic nonlinearity and the cumulative plastic deformation. These results demonstrate the feasibility of using nonlinear Rayleigh waves to characterize damage associated with plastic deformation, and this quantitative information can be a useful input for life prediction models.

1. Introduction

Cyclic loading and unloading of a steel structure leads to fatigue damage which can significantly weaken the structure's integrity and ultimately cause a catastrophic failure. Civil engineering structures tend to be large, complex, and unique in shape and are therefore expensive to repair or rebuild. This means that reliable and quantitative monitoring techniques are needed which are capable of characterizing fatigue damage before failure, so that adequate maintenance and repair actions can be taken in a timely manner.

Various ultrasonic nondestructive evaluation (NDE) techniques can be used for damage detection and characterization. Linear ultrasonic techniques are based on ultrasonic wave velocity, linear resonance frequency, or attenuation measurements. The sensitivity of these linear techniques, however, tends to be limited to the detection of relatively large defects such as macro-cracks and in general linear ultrasound cannot measure changes in material microstructure before the formation of macro-cracks. In contrast, nonlinear ultrasonic techniques have shown their capability to detect damage at the microstructure level in specimens undergoing fatigue and creep. These nonlinear acoustic techniques make use of the fact that during fatigue or creep, the dislocation density increases, which will create a nonlinear distortion of an ultrasonic wave that propagates through the material; this damage causes the generation of measurable higher harmonic components in an initially monochromatic ultrasonic signal. Nonlinear longitudinal waves have shown to be useful in characterizing creep damage [1] and have also been used to analyze fatigue damage in aluminum [2], pearlitic steels [3], and nickel-base superalloy [4]. Lamb waves have been applied to characterize the effects of fatigue damage [5]. Rayleigh surface waves have certain advantages over other wave types. Since the wave is generated and detected on the same side of a component, access to only one side of the component is required. Another useful characteristic of Rayleigh waves is that the energy is concentrated near the free surface. This makes Rayleigh waves ideal for applications where near-surface effects are important. It is known that fatigue cracks

* Corresponding author at: Georgia Institute of Technology, School of Civil and Environmental Engineering, MS 0355, Atlanta, GA 30332-0355, USA.
Tel.: +1 404 894 2344; fax: +1 404 894 0168.
E-mail address: laurence.jacobs@coe.gatech.edu (L.J. Jacobs).

0963-8695/$ - see front matter © 2012 Elsevier Ltd. All rights reserved.
doi:10.1016/j.ndteint.2012.02.002

initiate on the surface of a component, for example, the crack nucleation occurs mainly at the intersection of a persistent slip band with a boundary surface [6]. One way to detect a Rayleigh wave is with a laser interferometer system; this technique has been previously used to assess local fatigue damage in a titanium sample and to characterize damage in a nickel-base superalloy [7,8]. Other potential techniques include fluid coupled transducers [9] and the use of wedges to launch and detect Rayleigh surface waves [10].

The objective of this research is to use nonlinear Rayleigh surface waves to experimentally characterize the plasticity induced damage due to monotonic loading and cyclic low-cycle fatigue in A36 steel specimens. Three different specimens are subjected to quasi-static, monotonic tension, or cyclic fatigue loads, and the mechanical loading is interrupted to perform nonlinear ultrasonic measurements at a variety of intervals during the loading processes before the formation of macro-cracks. Wedge transducers are used to generate and detect nonlinear Rayleigh surface waves. The acoustic nonlinearity parameter is determined from the fundamental and second harmonic amplitudes, which are measured as a function of propagation distance. The measured acoustic nonlinearity parameters are plotted as a function of both the cumulative plastic strain and the number of fatigue cycles.

2. Theoretical background and methodology

In order to quantify acoustic nonlinearity, a nonlinear parameter for Rayleigh surface waves similar to the nonlinearity parameter for longitudinal waves is needed. Starting from the displacement potentials that describe the longitudinal and shear wave components, and using the fact that the acoustic nonlinearity for the shear wave vanishes in an isotropic material, the expression for the acoustic nonlinearity parameter β in terms of measured normal surface displacement components can be obtained [8]:

$$\beta = \frac{8u(2\omega)}{\omega^2 X u(\omega)^2} \frac{c_L\sqrt{c_L^2 - c_R^2}}{2(c_S/c_R)^2 - 1}, \quad (1)$$

where $u(\omega)$ and $u(2\omega)$ are the first and second order harmonic, out-of-plane displacement amplitudes at the free surface, X is the propagation distance of the Rayleigh wave, ω denotes the angular frequency, c_L, c_S, and c_R are the longitudinal, shear, and Rayleigh wave speeds, respectively. In this research, the fundamental frequency is held constant in all measurements, whereas the propagation distance is varied. The fundamental and second harmonic out-of-plane displacement amplitudes are measured for each propagation distance to obtain the normalized second harmonic $u(2\omega)/u(\omega)^2$ as a function of propagation distance. The slope of this function is proportional to the absolute acoustic nonlinearity parameter β, and is used as a relative acoustic nonlinearity parameter. An advantage of this approach to measure the acoustic nonlinearity parameter is that it is possible to isolate the material nonlinearity, which should increase linearly with increasing propagation distance, from the nonlinear effects of other sources such as electronic devices and transducers, which are constant with respect to propagation distance. In addition, this proposed measurement procedure is relatively simple to implement. The main source of variability is the coupling variation which occurs when attaching the wedge transducer at different locations along the path of propagation.

3. Specimens and mechanical testing

The material used in this research is standard carbon A36 steel. Flat dogbone specimens are machined from a single plate with a measured yield strain of 0.38%. The gauge section of the specimens has a length of 254 mm, a width of 25.4 mm, and a thickness of 6.35 mm which is 4.6 times larger than the Rayleigh wavelength at the fundamental frequency, 2.1 MHz, used in these experiments. The surfaces of the specimens are machine-ground to ensure smooth and consistent surface conditions. Both the quasi-static, monotonic, and fatigue tests are performed using a SATEC Uniframe servo hydraulic test frame and the strain is measured with an extensometer.

A single quasi-static, monotonic test specimen is loaded until a prescribed strain level, and immediately unloaded. The specimen is then removed from the test frame and the acoustic nonlinearity is measured for this strain level/damage state. The specimen is mounted back in the load frame and this procedure is repeated for the strain levels of 1.2%, 2.4%, 3.6%, and 4.8%. The mechanical load tests are performed using displacement control at a rate of 0.254 mm/s. No apparent necking occurs until a strain of 4.8% is reached. However, the quasi-static specimen failed during the next tensile loading without a further increase in plastic deformation with the exception of local strain in the necking area.

The fatigue tests are performed in tension–tension, load control mode, with a cycle rate of 0.5 Hz, and a constant maximum stress of 1.15 times the yield stress for the first fatigue specimen, and 1.16 times the yield stress for the second fatigue specimen. The stress ratio between minimum and maximum stress is chosen as 0.05 to make sure that the specimen does not undergo a compressive load. Since the maximum stress is above the yield stress, plastic deformation occurs even during the first cycle of each fatigue test. In a fashion similar to the monotonic tests, these fatigue tests are interrupted at a predetermined load cycle, and the specimen is removed for the ultrasonic measurements.

4. Ultrasonic measurement procedure

A schematic diagram of the experimental setup is shown in Fig. 1. Commercial piezoelectric longitudinal wave transducers are used to excite and detect the ultrasonic waves. The transducers are coupled to acrylic wedges, and these wedges are clamped to the A36 steel specimens. Light lubrication oil is used to couple the transducers to the wedges, as well as the wedges to the specimen. The center frequencies of the transmitting and receiving transducers (each a half inch in diameter) are 2.25 MHz and 5 MHz, respectively. The higher center frequency of the receiving transducer is selected to gain a higher sensitivity at the second harmonic frequency. A high power gated amplifier, RITEC RAM-5000 Mark IV is used to generate the tone burst input signal with a frequency of 2.1 MHz. In order to achieve a sufficiently large steady state portion, the length of the signal is 35 cycles; the transient portions in the beginning and end of the signal are

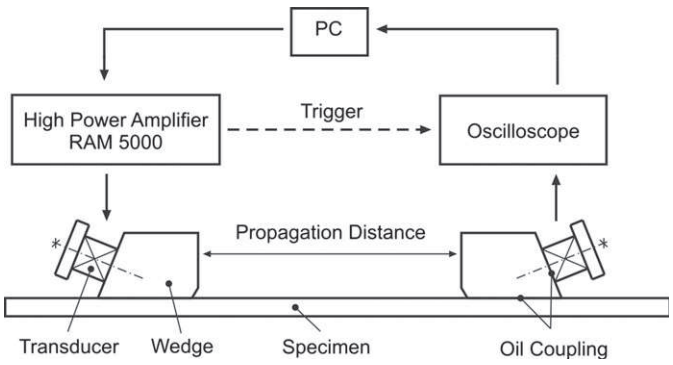

Fig. 1. Experimental setup for the ultrasonic measurements.

windowed out. 90% of the maximum available output level of the high power gated amplifier is used. The RITEC system is known for having a small inherent nonlinearity, creating a clean single frequency output. The time-domain signal received is recorded with an oscilloscope (Tektronix TDS 420) having a sampling rate of 100 MS/s, and to increase the signal to noise ratio (SNR) an average of 500 signals is used.

A typical measured time-domain signal (Rayleigh wave propagation distance of 8.5 cm) for an undamaged specimen is shown in Fig. 2(a). The first few cycles contain the turn-on transient effect and the last few cycles show the ringing effect. Before performing a Fast Fourier Transform (FFT), a Hann window is applied to the steady-state portion to eliminate these transient contributions. Fig. 2(b) shows the Fourier spectrum of the received signal. Note that different scales of the vertical axis are used for the fundamental and second harmonic. The uncalibrated amplitudes of the fundamental and second harmonic are called A_1 and A_2, respectively. The amplitude of the second harmonic is more than 20 times lower than the amplitude of the fundamental, but still well above the noise level with an SNR of about 25 dB at the second harmonic frequency (4.2 MHz). The amplitudes A_1 and A_2 are proportional to the out-of-plane displacement amplitudes, $u(\omega)$ and $u(2\omega)$. Therefore, the ratio A_2/A_1^2 is proportional to the absolute acoustic nonlinearity, β. This enables taking the slope of the linear fit of the normalized second harmonic amplitude plotted as a function of propagation distance, as a relative acoustic nonlinearity parameter.

Fig. 3 shows a plot of the normalized second harmonic amplitude as a function of propagation distance for an undamaged specimen. The ultrasonic measurements with respect to the propagation distance are repeated twice. In the second set of measurements, the transmitting wedge transducer is completely removed and re-attached, and these results are averaged and used to form the best linear fit shown in this plot. For small propagation distances, the near field of the transducer has a large influence on the results, while for large propagation distances (above 12 cm for these measurements), the geometric spreading and the attenuation due to the surface roughness plus material absorption lead to a leveling off and/or a decrease in the normalized second harmonic amplitude. Note that this same "leveling off" behavior is observed in shot peened aluminum specimens in [10] and can be partially attributed to surface conditions and the amount of material nonlinearity. For propagation distances between 7.5 cm and 11.5 cm, the linear relationship between the normalized second harmonic amplitude and the propagation distance given in Eq. (1) is clearly visible. Therefore, this range of propagation distances is used to determine the slope or acoustic nonlinearity parameter in the following measurements.

Since the measured acoustic nonlinearity for each of these different damage states will be compared, it is important to have an estimate of the error caused by this measurement procedure, specifically removing and replacing the transducers on the same specimen at different damage states. To address this, repeatability measurements are performed on an undamaged specimen and the results are shown in Fig. 4. Here, five sets of measurements

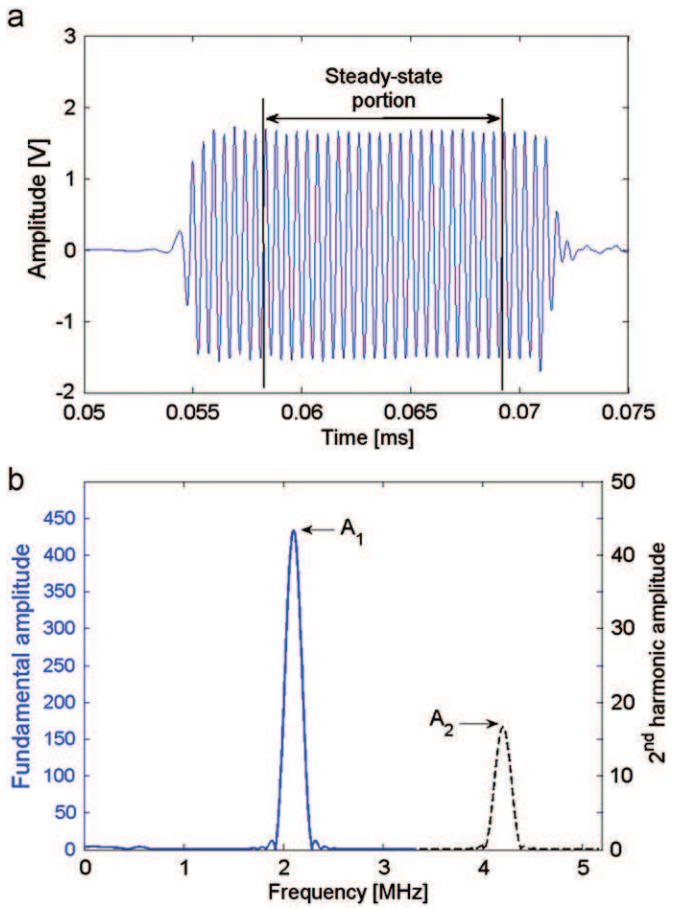

Fig. 2. (a) Typical time-domain signal and (b) its Fourier spectrum for an undamaged specimen (Rayleigh wave propagation distance of 8.5 cm).

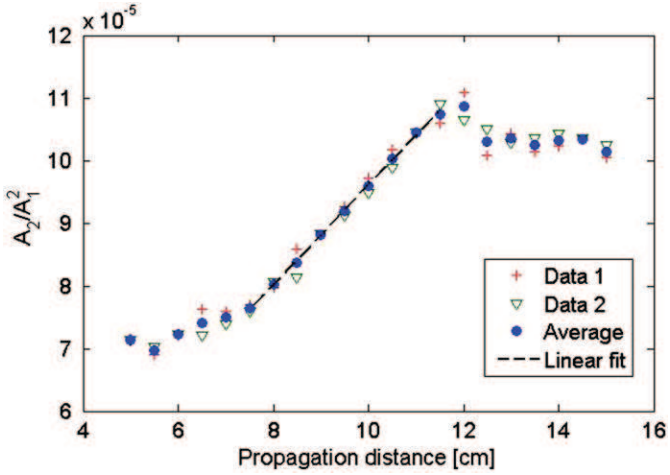

Fig. 3. Measured second harmonic amplitude normalized by the fundamental amplitude squared versus propagation distance for undamaged specimen.

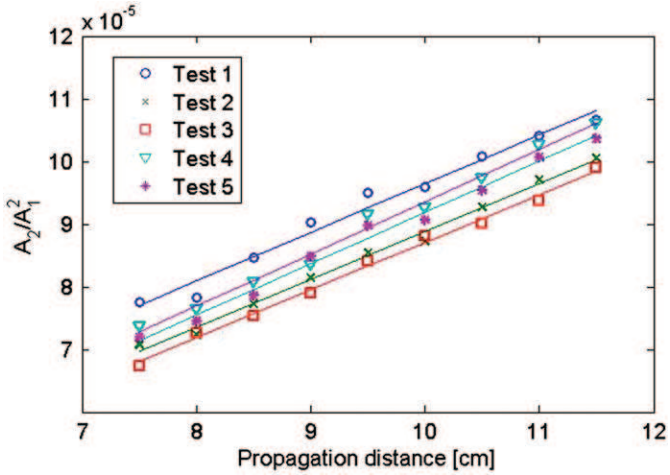

Fig. 4. Multiple results of the normalized second harmonic versus propagation distance for one damage state to show experimental repeatability.

are taken on the same specimen (in the same undamaged state), where the wedge transducers are completely removed and replaced for each measurement set. The slopes of the curves are found to be quite similar, demonstrating that the proposed nonlinear Rayleigh wave measurements are repeatable. The maximum and minimum slope values, which are the measured acoustic nonlinearities, vary by only +5.6% and −3.8% from the average. As a result, it can be estimated that the proposed ultrasonic measurement procedure introduces an error on the order of 10%.

5. Results

5.1. Quasi-static monotonic tension specimen

Fig. 5 shows the results of the ultrasonic measurements for the specimen subjected to a quasi-static, monotonic tension load, where the vertical axis shows the average value of the nonlinearity parameter normalized by its initial, undamaged value. This normalization is done by dividing all the measured nonlinearity parameters by that of the initial, undamaged specimen, and removes the uncertainty associated with the initial, undamaged material state, and better allows for comparisons between the different test specimens. For each damage state, the ultrasonic measurement is repeated 3–5 times, and the error bars represent the standard deviation of these measurements. The measured acoustic nonlinearity shows an increase for the first three strain levels, and reaches a maximum value of 30% above the value for the initial, undamaged state. The acoustic nonlinearity drops just before the specimen failure, or a total plastic strain of about 0.048. One reason for this drop at this high plastic strain level could be that, although no apparent necking occurred until the next strain level, the width of the specimen might have decreased enough to cause a geometric influence on the propagating Rayleigh wave. Overall, there is an increase in measured acoustic nonlinearity as a function of increasing plastic strain.

5.2. Fatigue specimens

Two A36 steel specimens are used to consider fatigue damage. First consider Fig. 6, which shows the normalized second harmonic amplitude, A_2/A_1^2 versus propagation distance for the first fatigue specimen in both its undamaged state, and after 88 load cycles (maximum for each load cycle is 1.15 times yield). The

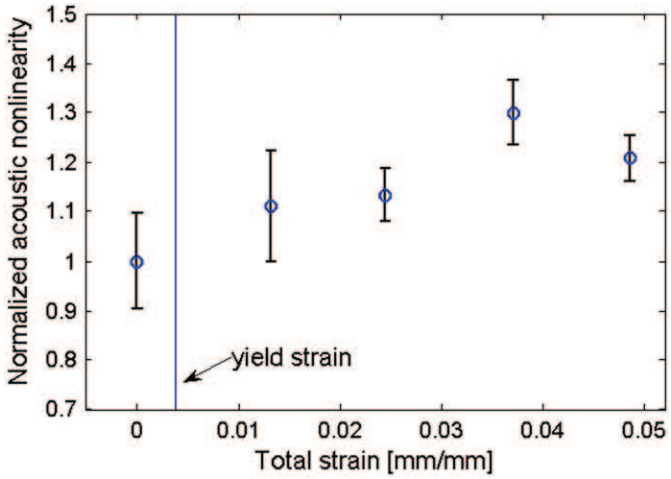

Fig. 5. Quasi-static, monotonic specimen, normalized acoustic nonlinearity versus total strain.

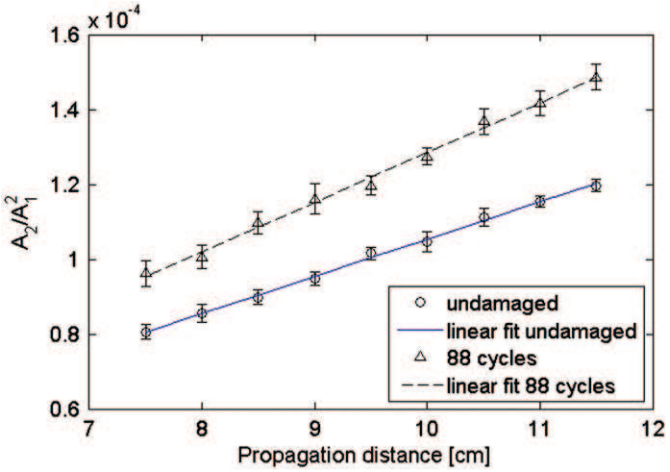

Fig. 6. Fatigue specimen 1, normalized second harmonic amplitude versus propagation distance for both the undamaged specimen and the same specimen after 88 fatigue cycles.

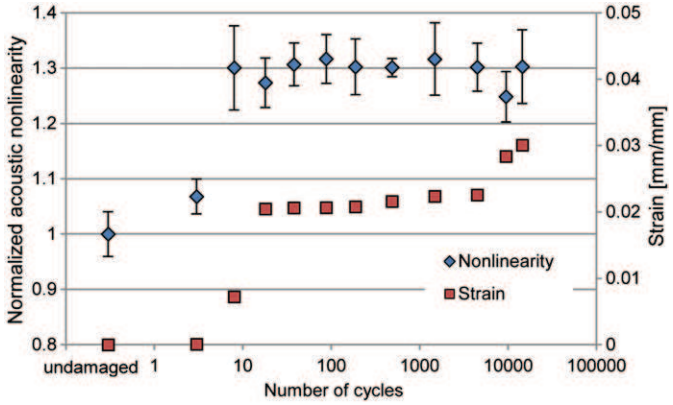

Fig. 7. Normalized acoustic nonlinearity and cumulative plastic strain versus number of fatigue cycles for fatigue specimen 1.

ultrasonic measurements are repeated at least three times at each propagation distance, which results in the error bars given. Note that these error bars are small, which shows the consistent repeatability of these ultrasonic measurements. The fact that the measured acoustic nonlinearity is still linear, as a function of propagation distance, after the specimen has experienced 88 fatigue cycles indicates that the fatigue damage is fairly uniformly distributed throughout the section of the specimen under consideration at this damage state. Most importantly, this plot shows that the slope of the linear fit for the specimen after the damage of 88 cycles is higher than in its initial, undamaged state.

Figs. 7 and 8 show the measured acoustic nonlinearity and the cumulative plastic strain, for each specimen, as a function of load cycle, or damage state. In both cases the acoustic nonlinearity parameter is again normalized by the initial, undamaged value. The error bars result from 3–5 repeated ultrasonic measurements on each specimen. For the first specimen, the nonlinearity parameter shows a large increase in the first eight load cycles. After more than 100 load cycles, no further increase in acoustic nonlinearity is observed; this acoustic nonlinearity remains almost constant at 30% above the nonlinearity parameter of its undamaged state. The second specimen (Fig. 8) also shows an increasing trend at the beginning, followed by a leveling off of the acoustic nonlinearity with an increase in number of load cycles. However, the magnitude of this acoustic nonlinearity is lower than that for the first specimen, and this curve shows a slight

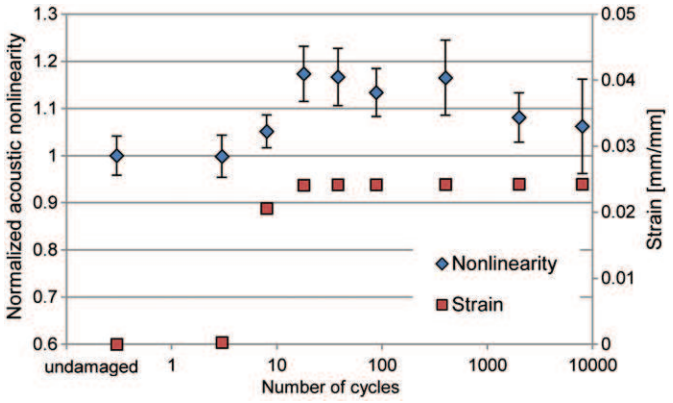

Fig. 8. Normalized acoustic nonlinearity and cumulative plastic strain versus number of fatigue cycles for fatigue specimen 2.

decrease above 1000 load cycles. A similar leveling off or "saturation" of the measured acoustic nonlinearity later in the fatigue life (after an initial increase) has also been observed in the results from specimens in other materials, such as a nickel-base superalloy [4] and aluminum [5]. How early this saturation occurs depends on the microstructure, and the elastic–plastic properties of a material.

Figs. 7 and 8 also show that the behavior of the measured acoustic nonlinearity is clearly related to the amount of plastic deformation measured with the extensometer during fatigue. During the first number of load cycles, the amount of plastic strain is high. However, at the later stages of fatigue the additional plastic strain at each cycle levels off and stabilizes. This behavior is consistent with experimental results in other materials with a variety of loading conditions [1–10], and adds additional credence to the conclusion that the measured acoustic nonlinearity is plasticity driven. An increase in plastic deformation leads to a large increase in the acoustic nonlinearity. However, the microstructural changes during these later load cycles do not cause significant changes in the acoustic nonlinearity of A36 steel. This is an important observation in that the cumulative plastic strain is often used as a direct measure or indicator of fatigue damage in a component subjected to high external loads. Since this nondestructively determined acoustic nonlinearity is closely related to the plastic strain, this directly measurable parameter can be used also as a direct measure of fatigue damage accumulated in a component. This relationship is important and useful in the remaining lifetime prediction models based on accumulated plastic damage.

The saturation of the acoustic nonlinearity parameter during fatigue can be explained using a well-accepted description of the microstructure evolution during fatigue [11]. When a metallic specimen is subjected to cyclic loading, the cyclic hardening/softening first occurs. During this initial period, a vast amount of dislocations are newly generated which leads to the hardening/softening as a macroscopic manifestation of the dislocation generation. These newly generated dislocations will then form substructural organizations such as veins and persistent slip bands (PSBs). Veins are the channels through which dislocations move, and the PSBs are where the moving dislocations are piled up in a certain regular geometric shape (such as a ladder structure). Therefore, in the initial stage of fatigue, the acoustic nonlinearity (in response to the dislocations) increases monotonically as is seen in this research and also other existing work. The dislocation-rich volumes such as those that contain PSBs are more compliant, and thus can take much of the external load. As the fatigue progresses, the stress due to the external load is concentrated, and thus the strain is localized at certain locations where the dislocation density is higher, while the strain in other areas of the specimen is relaxed. This strain relaxation slows down the generation of new dislocations—so, the acoustic nonlinearity is now saturated. Therefore, the saturation phenomenon is closely related to the strain localization, and thus the crack nucleation/initiation. At the locations with high strain and dislocations substructures, cracks will eventually nucleate with the further progress of fatigue. Finally, one dominant crack will grow to a macrocrack that can lead to specimen failure.

6. Conclusion

This research presents an ultrasonic technique to characterize damage due to quasi-static, monotonic tension, and fatigue in A36 steel in which changes in the acoustic nonlinearity are measured. Nonlinear Rayleigh surface waves are generated and detected using a wedge technique, and these measurements are shown to be efficient and repeatable. The expected linear relationship between the normalized second harmonic amplitude A_2/A_1^2 and the propagation distance is observed for a certain range of propagation distances. This allows for using the slope of the linear fit as a relative acoustic nonlinearity parameter. The acoustic nonlinearity increases with plastic strain for A36 steel during monotonic loading. In addition, the influence of fatigue on the acoustic nonlinearity is observed. It is shown that for A36 steel, the acoustic nonlinearity rapidly increases during the first few fatigue cycles when the maximum load is above the yield stress (low cycle fatigue). However, for higher numbers of cycles, no further increase in the acoustic nonlinearity is observed. These results indicate that the acoustic nonlinearity for A36 steel is highly dependent on plastic deformation, since during the fatigue test most of the plastic deformation occurs within the first few cycles. Note that the results and interpretations in this research are specifically for the case of low cycle fatigue. It will be also interesting to perform similar measurements for high- and medium-cycle fatigue cases which will be considered in future research.

The issues of the proposed measurement technique are the high sensitivity to changes in the surface condition and the difficulty in maintaining consistent coupling conditions. However, its advantages are the relatively simple measurement setup with acrylic wedges and the fact that the measured nonlinearity solely results from material nonlinearity, whereas the system nonlinearity is eliminated.

Acknowledgments

The authors would like to thank the Deutscher Akademischer Austauschdienst (DAAD) for providing partial financial support.

References

[1] Valluri JS, Balasubramaniam K, Prakash RV. Creep damage characterization using non-linear ultrasonic techniques. Acta Mater 2010;58:2079–90.
[2] Cantrell JH, Yost WT. Nonlinear ultrasonic characterization of fatigue microstructures. Int J Fatigue 2001;23:487–90.
[3] Sagar SP, Metya AK, Ghosh M, Sivaprasad S. Effect of microstructure on nonlinear behavior of ultrasound during low cycle fatigue of pearlitic steels. Mater Sci Eng A—structural Materials Properties Microstructure and Processing 2011;528:2895–8.
[4] Kim J-Y, Jacobs LJ, Qu J. Experimental characterization of fatigue damage in a nickel-base superalloy using nonlinear ultrasonic waves. J Acoust Soc Am 2006;120(3):1266–73.
[5] Pruell C, Kim J-Y, Qu J, Jacobs LJ. Evaluation of fatigue damage using nonlinear guided waves. Smart Mater Struct 2009;18:035003.

[6] Kim WH, Laird C. Crack nucleation and stage I propagation in high strain fatigue-I. Microscopic and interferometric observations. Acta Metall 1978;26:777–87.
[7] Blackshire JL, Sathish S, Na J, Frouin J. Nonlinear laser ultrasonic measurements of localized fatigue damage. Rev Prog Quant Nondestr Eval 2003;22: 1479–88.
[8] Herrmann J, Kim J-Y, Jacobs LJ, Qu J, Littles JW, Savage MF. Assessment of material damage in a nickel-base superalloy using nonlinear Rayleigh surface waves. J Appl Phys 2006;99(12).
[9] Barnard DJ, Brasche LJH, Raulerson D, Degtyar AD. Monitoring fatigue damage accumulation with Rayleigh wave harmonic generation measurements. Rev Prog Quant Nondestr Eval 2003;22:1393–400.
[10] Liu M, Kim J-Y, Jacobs L, Qu J. Experimental study of nonlinear Rayleigh wave propagation in shot-peened aluminum plates—feasibilty of measuring residual stress. NDT&E Int 2010;44:67–74.
[11] Suresh S. Fatigue of materials. Cambridge solid state science series. Cambridge University Press; 1998.